Focal adhesion kinase links mechanical force to skin fibrosis via inflammatory signaling

Victor W. Wong, Kristine C. Rustad, Satoshi Akaishi, Michael Sorkin, Jason P. Glotzbach, Michael Januszyk, Emily R. Nelson, Kemal Levi, Josemaria Paterno, Ivan N. Vial, Anna A. Kuang, Michael T. Longaker, Geoffrey C. Gurtner

Supplementary Figure 1

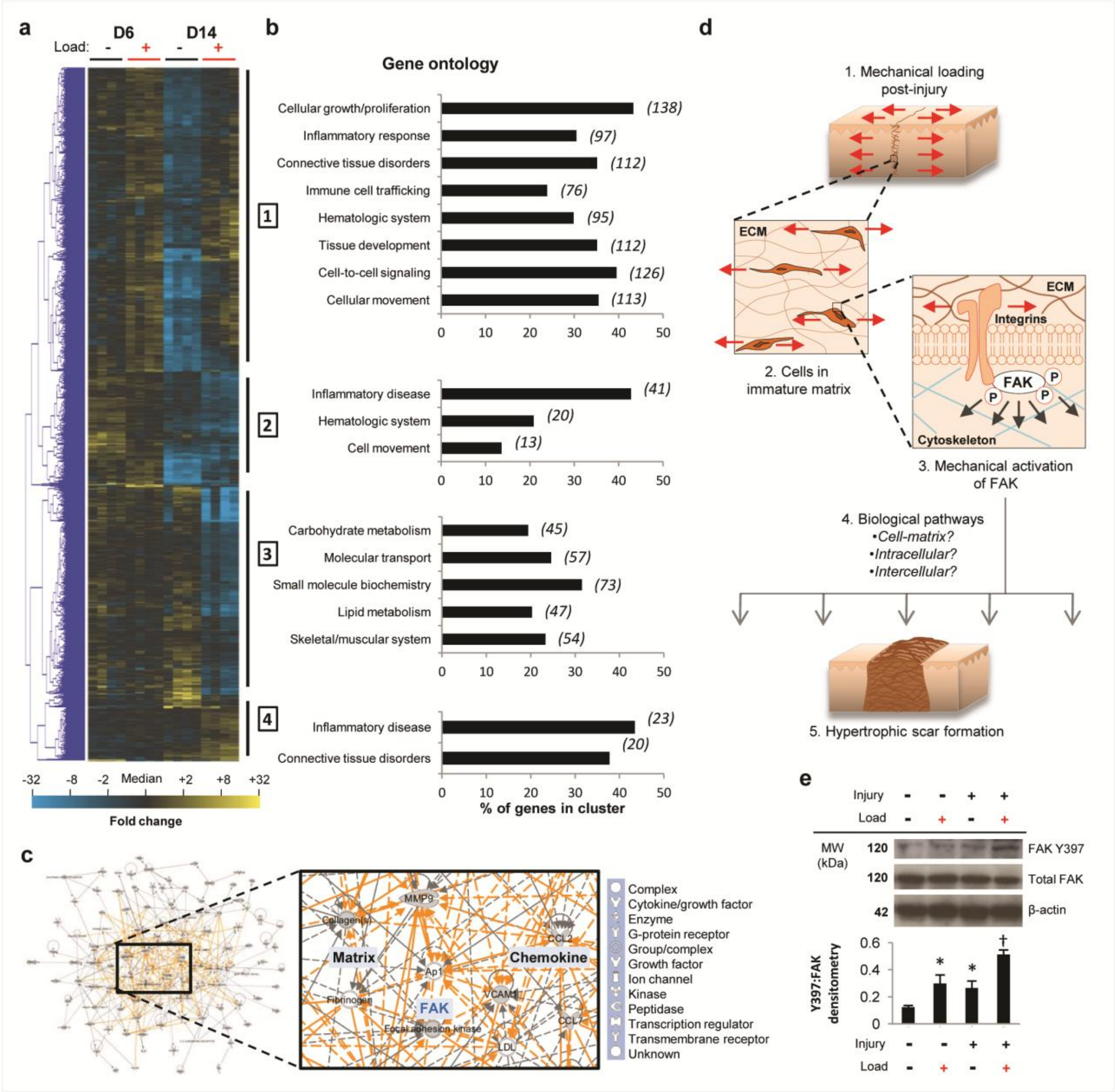

Nature Medicine doi:10.1038/nm.2574

Microarray analysis of HTS formation. Wildtype wounds at day 6 (±48 hours loading) and day 14 post-injury (±10 days loading) were analyzed. (**a**) Hierarchical clustering of 1,046 differentially expressed genes (day 6=189 genes, day 14=847 genes, both day 6 and 14=73 genes). Rows=genes; columns=samples (n=4/group). Yellow and blue indicate up- and down-regulation, respectively. (**b**) Gene ontology categories significantly altered by loading. Number of genes/category italicized. (**c**) Ingenuity Pathways Analysis-constructed transcriptome networks. Solid=direct; dashed=indirect interactions; orange=internetwork connections. (**d**) Schematic of potential mechanotransduction pathways in fibrosis. (**e**) Immunoblot quantification of FAK activation following injury and/or loading. n=3. Values represent means ± s.e.m.; *p=0.05, †p<0.001.

Supplementary Figure 2

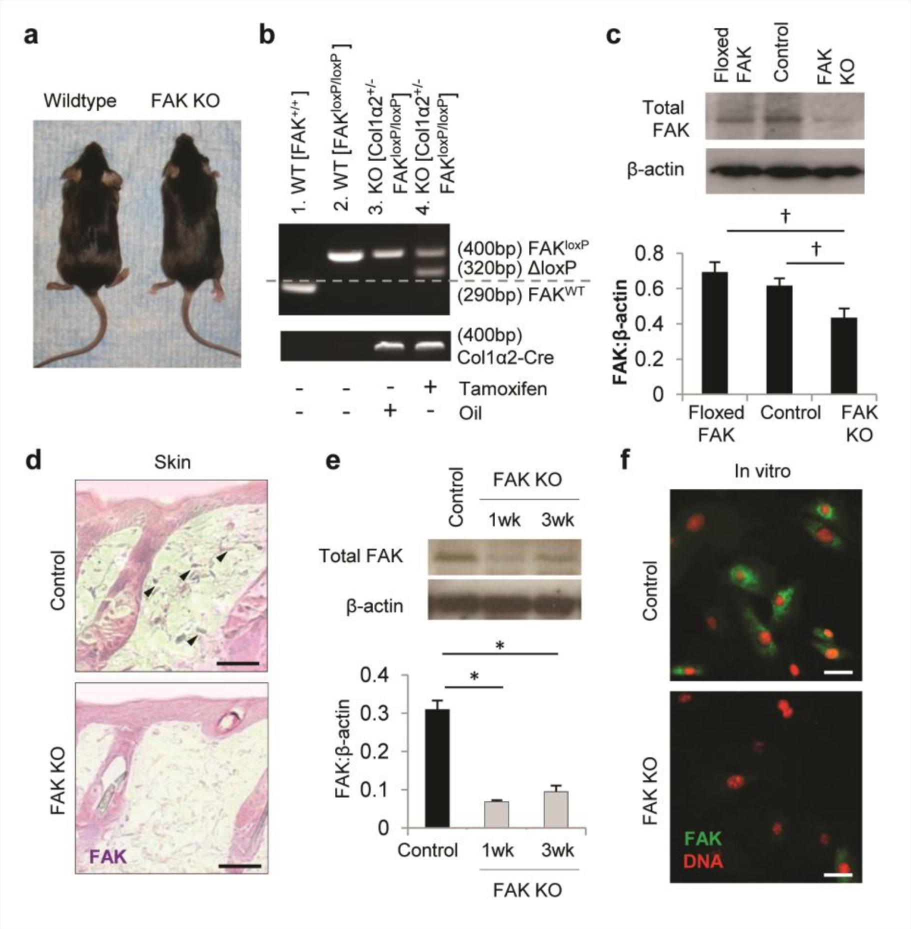

Validation of FAK KO mice. (**a**) Photograph of age-matched wildtype and FAK KO mice. (**b**) PCR confirmation of tamoxifen-dependent excisive recombination of FAK. ‘FAK^{loxP}’ is floxed FAK band, ‘ΔloxP’ is recombined band after FAK excision, ‘FAK^{WT}’ is wildtype band. (**c**) Quantification of FAK densitometry from unwounded skin. n=6. (**d**) Immunolocalization of FAK in unwounded skin. Arrowheads point to dermal FAK signal. Scale bar 50 μm. (**e**) Quantification of FAK densitometry from harvested primary dermal fibroblasts at 1 and 3 weeks post-tamoxifen induction. n=6. (**f**) FAK immunofluorescence images of adult dermal fibroblasts in vitro. Scale bar 50 μm. Values represent means ± s.e.m. *$p<0.001$; †$p<0.01$.

Supplementary Figure 3

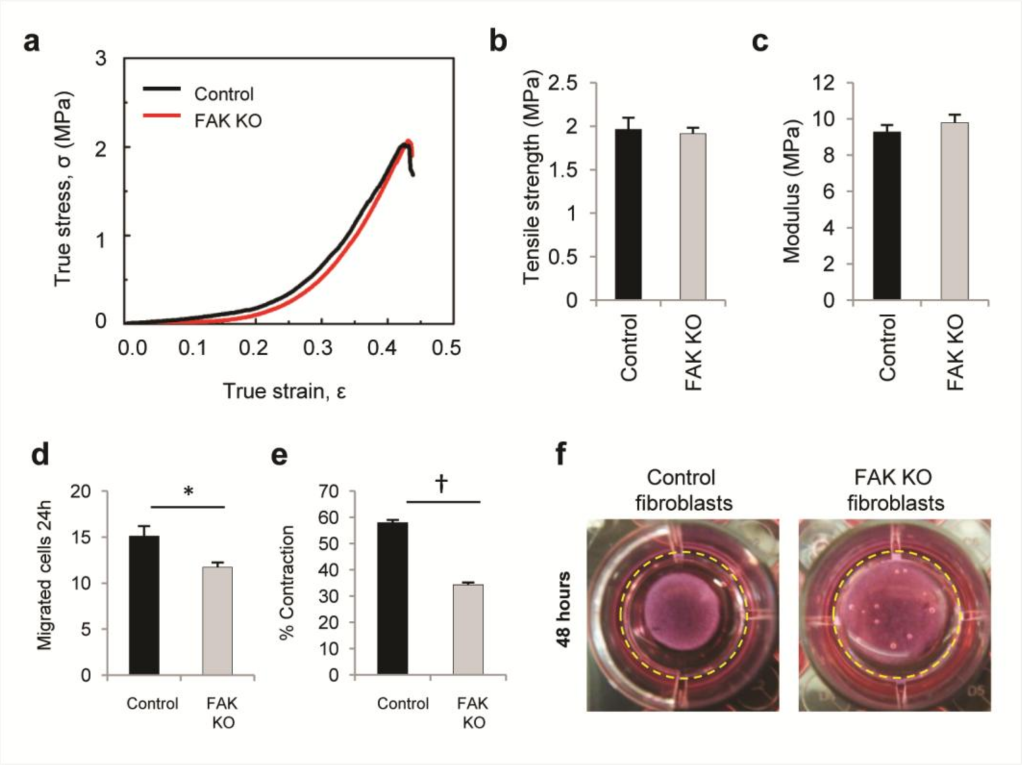

Studying FAK mechanotransduction. (**a**) Representative stress-strain profile of day 10 incisions from FAK KO (red) and control (black) mice. (**b**) Ultimate tensile strength and (**c**) wound stiffness were similar between control and FAK KO incisions. n=4. In vitro migration and contraction assays. (**d**) Primary dermal fibroblasts harvested from FAK KO mice demonstrated impaired motility after 24 hours in a scratch migration assay. n=14. (**e**) FAK KO fibroblasts also demonstrated a significant reduction in contraction in 3D collagen lattices after 48 hours. n=9. (**f**) Representative photographs of collagen lattices for the respective conditions. Values represent means ± s.e.m. *$p<0.01$; †$p<0.001$.

Nature Medicine doi:10.1038/nm.2574

Supplementary Figure 4

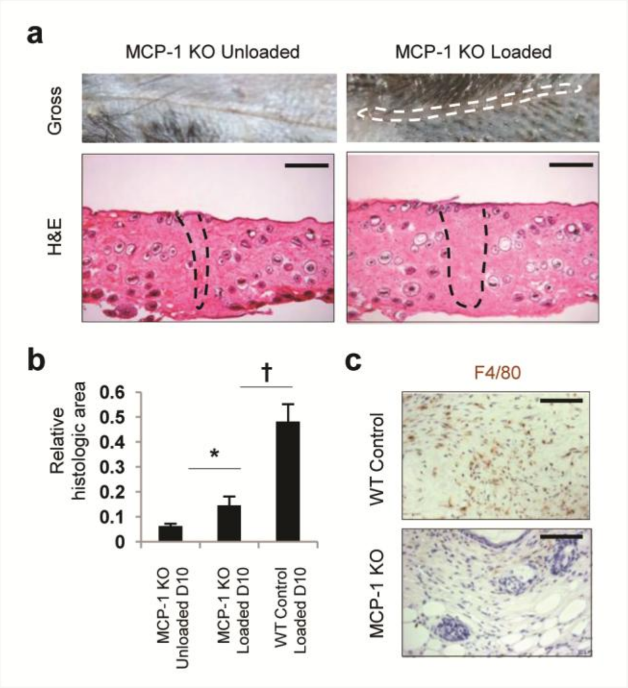

Application of HTS model to MCP-1 KO mice. (**a**) Representative gross and H&E-stained histologic images of unloaded and loaded scars at day 10 post-injury in global MCP-1 KO mice. Dashed line demarcates scar boundary. n=6. (**b**) Quantification of histologic scar area. (**c**) Immunolocalization of F4/80+ macrophages. n=6. Scale bar 100 µm. Values represent means ± s.e.m.; scale bar 0.5 cm gross photographs; 200 µm in a and c. *p<0.05; †p<0.01.

Supplementary Figure 5

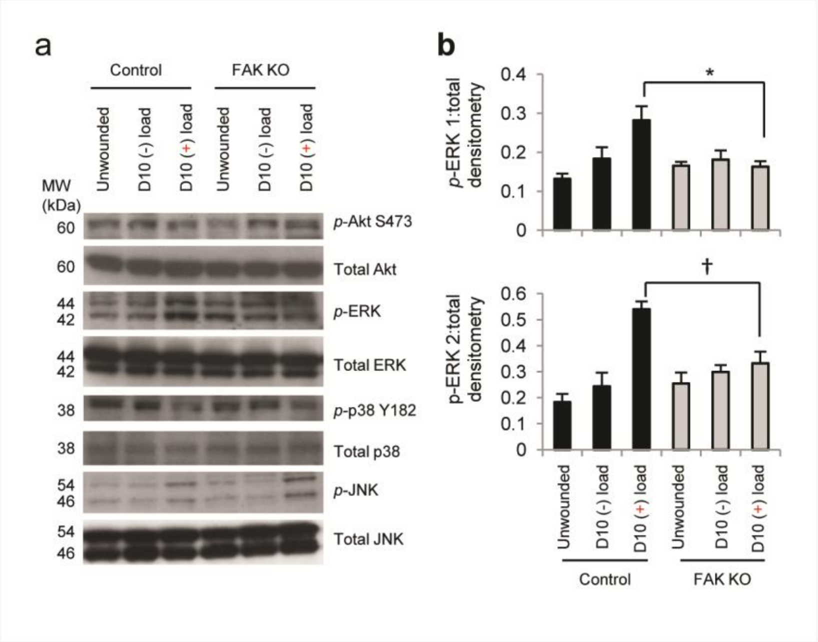

Immunoblot analysis of mechanotransduction pathways in scar formation. (**a**) Representative immunoblots of unwounded skin, unloaded incisions and loaded scars in control and FAK KO mice. The intracellular kinases Akt, ERK, p38 and JNK are suspected downstream mediators of FAK signaling. (**b**) Only ERK activation was differentially regulated by FAK mechanotransduction, implicating a potential FAK-ERK axis in the mechanical induction of fibrosis and scar formation. Values represent means ± s.e.m. n=3. $^*p<0.05$, $^\dagger p<0.01$.

Supplementary Figure 6

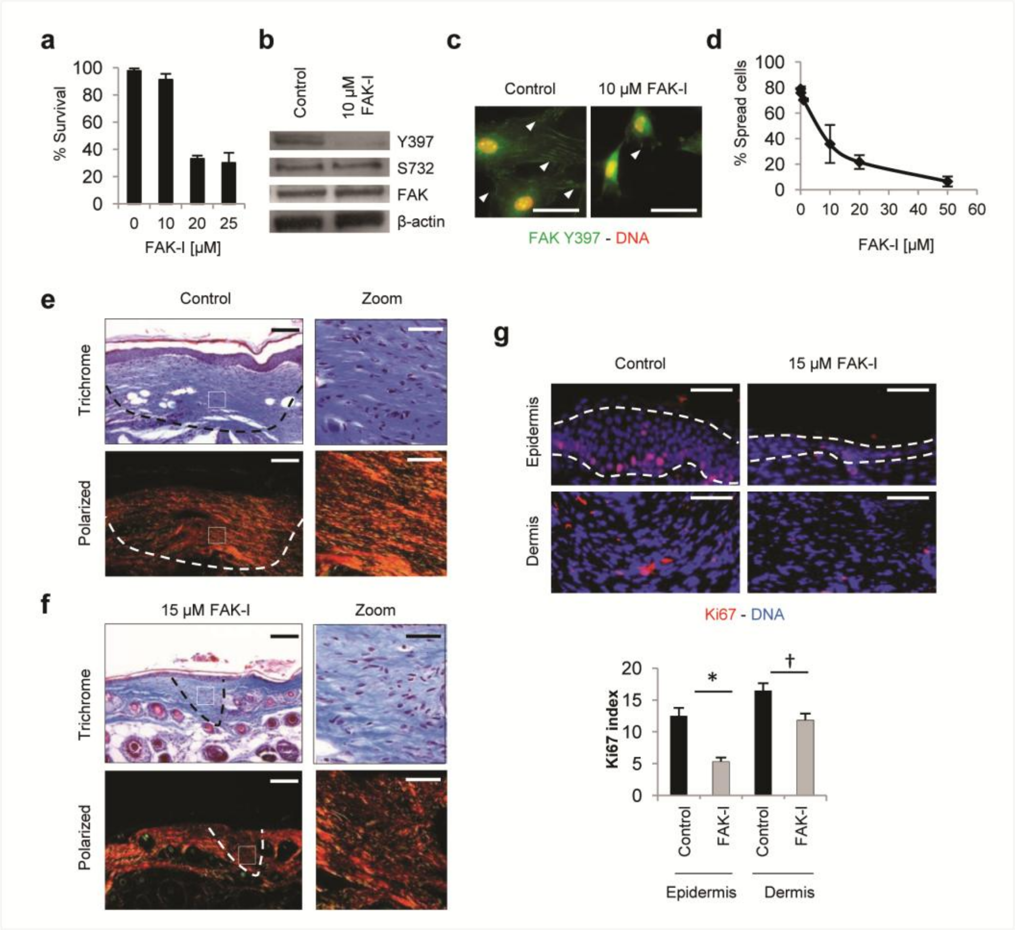

Small molecule inhibition of FAK using PF573228 in vitro and in vivo. (**a**) Fibroblast survival based on live/dead assay following different doses of PF573228. (**b**) Immunoblot demonstrating FAK Y397 specificity. FAK activation at S732 is not impaired. (**c**) PF573228 markedly impairs immunolocalization of FAK Y397 (arrowheads) in plated fibroblasts. Scale bar 50 μm. (**d**) Fibroblast morphology and attachment is impaired with application of PF573228. (**e–f**) Trichrome-stained and polarized light analysis of FAK inhibitor-treated scars at day 10 post-injury. Dashed line demarcates scar boundary. Scale bar 100 μm (zoom is 20 μm). (**g**) Quantification of scar proliferation (% of Ki67+ cells). Dashed line outlines epidermis. n=6. Values represent means ± s.e.m.; *$p<0.01$, †$p<0.05$.

Supplementary Figure 7

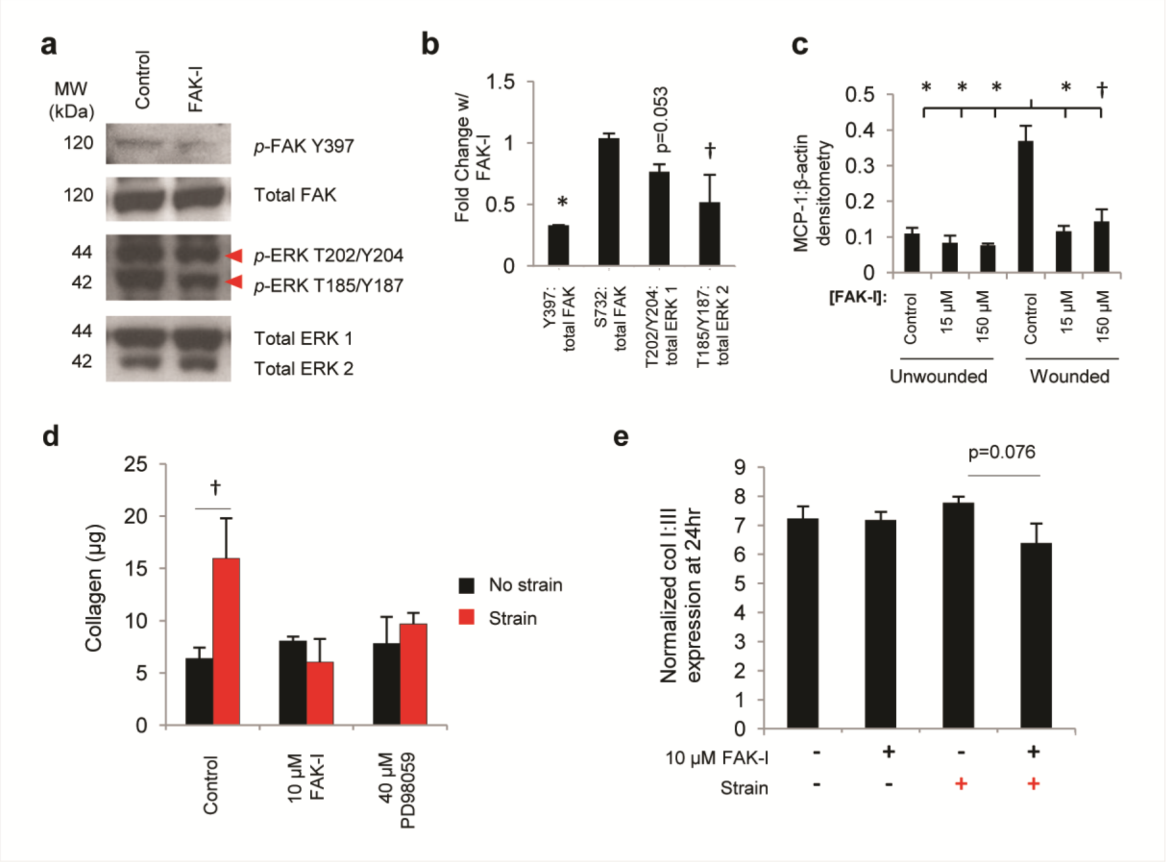

Small molecule inhibition of FAK-mediated pathways. (**a–b**) Immunoblot analysis of FAK and ERK activation in post-injury day 10 scars. Red arrowheads point to decreased ERK phosphorylation. Fold change represents values relative to vehicle injection. n=4. (**c**) Immunoblot analysis of MCP-1 levels following application of small molecule FAK inhibitor in vivo. n=3. (**d**) 24 hours of mechanical strain activated human fibroblast secretion of total collagen in vitro. Inhibition of FAK (PF573228) or ERK (PD98059) significantly blocked this effect. n=4. (**e**) Strain-induced human fibroblast gene expression of collagen I (thicker):collagen III (thinner) with inhibition of FAK. Values normalized to β-actin. n=6. Values represent means ± s.e.m. *p<0.01, †p<0.05.

Supplementary Table 1: Microarray-based list of 73 gene targets significantly regulated by mechanical loading at both day 6 and day 14 post-injury (false discovery rate < 2 for both time points).

Gene		**Fold change**	
		Day 6	**Day 14**
Adam12	ADAM metallopeptidase domain 12	2.28	10.09
Agpat9	1-acylglycerol-3-phosphate O-acyltransferase 9	0.58	0.24
Akr1b15	aldo-keto reductase family 1, member B15	1.51	3.23
Arsi	arylsulfatase family, member I	2.18	2.45
Bgn	biglycan	1.52	3.37
Ccr5	chemokine (C-C motif) receptor 5	1.49	2.02
Ckap4	cytoskeleton-associated protein 4	2.02	3.05
Clec11a	C-type lectin domain family 11, member A	2.17	3.99
Col14a1	collagen, type XIV, alpha 1	1.95	3.75
Col1a2	collagen, type I, alpha 2	1.89	4.59
Col5a1	collagen, type V, alpha 1	1.64	6.83
Col5a2	collagen, type V, alpha 2	1.63	9.06
Col8a1	collagen, type VIII, alpha 1	2.52	29.35
Csgalnact1	chondroitin sulfate N-acetylgalactosaminyltransferase 1	1.97	1.98
Csrp2	cysteine and glycine-rich protein 2	2.32	5.15
D14ertd668e	DNA segment, Chr 14, ERATO Doi 668, expressed	1.89	1.71
Dact1	dapper, antagonist of beta-catenin, homolog 1 (Xenopus laevis)	1.90	3.01
Ddah1	dimethylarginine dimethylaminohydrolase 1	2.16	6.88
Dpysl3	dihydropyrimidinase-like 3	2.02	2.99
Dst	dystonin	0.59	0.45
Dusp13	dual specificity phosphatase 13	0.46	0.45
Dysfip1	dysferlin interacting protein 1	0.47	0.21
Edil3	EGF-like repeats and discoidin I-like domains 3	2.20	2.36
Efemp2	EGF-containing fibulin-like extracellular matrix protein 2	1.73	3.11
Emilin1	elastin microfibril interfacer 1	2.02	6.42
Epb41l3	erythrocyte membrane protein band 4.1-like 3	1.56	2.45
F2r	coagulation factor II (thrombin) receptor	1.62	3.25

Fam114a1	family with sequence similarity 114, member A1	1.53	3.91
Fam134b	family with sequence similarity 134, member B	0.63	0.39
Fbn1	fibrillin 1	1.91	5.84
Fbn2	fibrillin 2	2.27	9.52
Fibin	fin bud initiation factor homolog (zebrafish)	2.16	3.05
Fkbp14	FK506 binding protein 14, 22 kDa	1.72	3.55
Fn1	fibronectin 1	2.02	2.89
Galntl1	UDP-N-acetyl-alpha-D-galactosamine:polypeptide N-acetylgalactosaminyltransferase-like 1	1.65	2.04
Glis3	GLIS family zinc finger 3	2.14	1.85
Hif1a	hypoxia inducible factor 1, alpha subunit (basic helix-loop-helix transcription factor)	1.46	3.83
Igf1	insulin-like growth factor 1 (somatomedin C)	1.88	5.00
Ikbip	IKBKB interacting protein	1.41	3.35
Il1rl1	interleukin 1 receptor-like 1	3.82	2.99
Islr	immunoglobulin superfamily containing leucine-rich repeat	1.78	2.85
Kdelr3	KDEL (Lys-Asp-Glu-Leu) endoplasmic reticulum protein retention receptor 3	1.53	4.88
Leprel2	leprecan-like 2	1.75	6.49
Loxl1	lysyl oxidase-like 1	1.63	4.30
Loxl2	lysyl oxidase-like 2	1.71	5.45
Lsp1	lymphocyte-specific protein 1	1.57	2.91
Ltbp2	latent transforming growth factor beta binding protein 2	2.71	3.04
Meg3	maternally expressed 3	1.49	11.80
Mest	mesoderm specific transcript homolog (mouse)	4.07	8.41
Mfap4	microfibrillar-associated protein 4	1.90	9.05
Mfap5	microfibrillar associated protein 5	3.03	3.39
Mirg	miRNA containing gene	1.62	2.87
Mmp19	matrix metallopeptidase 19	2.21	1.80
Mmp23b	matrix metallopeptidase 23B	1.56	3.60
Mrc2	mannose receptor, C type 2	1.66	3.11
Nid1	nidogen 1	1.59	4.25
Nov	nephroblastoma overexpressed gene	2.83	23.44
Oaf	OAF homolog (Drosophila)	1.84	2.30
P4ha3	prolyl 4-hydroxylase, alpha polypeptide III	2.55	3.23
Plat	plasminogen activator, tissue	1.83	3.66

Prrx2	paired related homeobox 2	1.61	2.74
Ptx3	pentraxin 3, long	3.02	8.50
Pycr1	pyrroline-5-carboxylate reductase 1	1.64	2.82
Rffl	ring finger and FYVE-like domain containing 1	0.66	0.31
Serpinh1	serpin peptidase inhibitor, clade H (heat shock protein 47), member 1, (collagen binding protein 1)	1.70	2.52
Slc39a14	solute carrier family 39 (zinc transporter), member 14	1.58	1.77
Srpx2	sushi-repeat-containing protein, X-linked 2	2.16	6.68
Timp1	TIMP metallopeptidase inhibitor 1	2.71	10.04
Tnc	tenascin C	2.36	9.30
Tnn	tenascin N	3.43	10.51
Vcan	versican	2.00	3.36
Wisp1	WNT1 inducible signaling pathway protein 1	2.04	9.68
Zfpm2	zinc finger protein, multitype 2	2.77	1.97

Supplementary Table 2: Microarray-identified chemokine genes that are significantly regulated by mechanical loading (false discovery rate < 2 for at least one time point).

Gene		Fold change	
		Day 6	Day 14
Ccl11	chemokine (C-C motif) ligand 11	2.92	1.66
Ccl2	chemokine (C-C motif) ligand 2	2.44	3.42
Ccl7	chemokine (C-C motif) ligand 7	2.61	2.92
Ccl8	chemokine (C-C motif) ligand 8	1.45	2.34
Ccr1	chemokine (C-C motif) receptor 1	1.22	5.03
Ccr2	chemokine (C-C motif) receptor 2	1.30	2.89
Ccr5	chemokine (C-C motif) receptor 5	1.49	2.02
Cxcl1	chemokine (C-X-C motif) ligand 1	2.44	1.49
Cxcl16	chemokine (C-X-C motif) ligand 16	1.05	1.85
Cmtm7	CKLF-like MARVEL transmembrane domain containing 7	1.50	1.69
Csf1r	colony stimulating factor 1 receptor	1.09	2.73
Csf2ra	colony stimulating factor 2 receptor, alpha, low-affinity (granulocyte-macrophage)	1.13	1.72
Hif1a	hypoxia inducible factor 1, alpha subunit	1.46	3.83
Il13ra1	interleukin 13 receptor, alpha 1	1.16	2.49
Il1rl1	interleukin 1 receptor-like 1	3.82	2.99
Il27ra	interleukin 27 receptor, alpha	1.27	1.47
Il2rg	interleukin 2 receptor, gamma chain	1.33	2.39
Il33	interleukin 33	2.24	7.31
Il4ra	interleukin 4 receptor, alpha	1.64	1.92
Lif	leukemia inhibitory factor	1.82	1.39
Ltbp2	latent transforming growth factor beta binding protein 2	2.71	3.04
Mmp2	matrix metallopeptidase 2	1.29	2.50
Mmp9	matrix metallopeptidase 9	1.37	2.16
Nfkbie	nuclear factor of kappa light polypeptide gene enhancer in B-cells inhibitor, epsilon	1.34	2.26
Rgs5	regulator of G-protein signaling 5	0.78	3.93
Tlr1	toll-like receptor 1	1.24	2.72
Tlr13	toll-like receptor 13	1.29	3.03
Tnfaip6	tumor necrosis factor alpha induced protein 6	2.39	1.46
Tnfrsf1b	tumor necrosis factor receptor superfamily, member 1b	1.20	2.05
Trem2	triggering receptor expressed on myeloid cells 2	1.28	2.47

Supplementary Table 3: qPCR primer list for mouse genes and qPCR Taqman assays for human genes.

Mouse Gene	**Forward Primer 5' → 3'**	**Reverse Primer 5' → 3'**
Col1a1	GCTGTTCTTGCAGTGATAGGTG	CTGGTTTGGAGAGAGCATGAC
Col3a1	CATTCCTCCCACTCCAGACTT	CTGTGAATCATGTCCAACTGGT
Ccl2	AATGAGTAGCAGCAGGTGAGTG	GAAGCCAGCTCTCTCTTCCTC
Ctgf	CGCAGAACTTAGCCCTGTATGT	GCTGACCTGGAGGAAAACATTA
Tgfb1	ATCTTTGCTGTCACAAGAGCAG	TCTTTTGACGTCACTGGAGTTG
Tgfb3	TGAAAGGTGTGACATGGACAGT	CGCTACATAGGTGGCAAGAATC
Mmp2	GCATCTACTTGCTGGACATCAG	AGGAGGAGAAGGCTGTGTTCTT
Mmp9	TGGGAGGTATAGTGGGACACAT	GCTTCCCTCTGAATAAAGACGA
Actb	ATGTTCAATGGGGTACTTCAGG	CTGTATTCCCCTCCATCGTG

Human Gene	**Taqman assay**
COL1A1	Hs00164004_m1
COL3A1	Hs00943809_m1
ACTB	Hs9999903_m1